Open access Journal International Journal of Emerging Trends in Science and Technology

A New Technique for Power Quality Improvement Using D-statcom By Back-Propagation Control Algorithm

Authors
Raja.Sai Kiran[1], Mr. M.Nagaraju[2]
[1]PG Student [EPS], Dept. of EEE, ASIT, Gudur, SPSR Nellore (D), Andhra Pradesh, India
[2]Associate Professor, Dept. of EEE, ASIT, Gudur, SPSR Nellore (D), Andhra Pradesh, India

Abstract
In this paper by using a back propagation (BP) control algorithm we will implement a three phase distribution static compensator (DSTATCOM) for its functions such as load balancing, harmonic elimination, and reactive power compensation or power factor correction, and zero voltage regulation under nonlinear loads. A BP-based control algorithm is used for the estimation of reference source currents by extraction of the fundamental weighted value of active and reactive power components of load currents. Using a digital signal processor we will develop a prototype for DSTATCOM, and its performance is analyzed under various operating conditions. The performance of DSTATCOM is found to be satisfactory with the proposed control algorithm for various types of loads.

Index Terms—*Back propagation (BP) control algorithm, harmonics, load balancing, power quality, weights.*

I. INTRODUCTION

Power quality improvement have become increasingly important due to the intensive use of power converters and other nonlinear loads which results in the deterioration of power system voltages and current waveforms. Thus the current wave form can become quite complex depending up on the type of load and its interaction with other components in the system. One of the major effects of power system harmonics is to increase the current in the system. It also causes other problems like greater power losses in distribution and operation failure of protection devices. THE QUALITY of available supply power has a direct economic impact on industrial and domestic sectors which affects the growth of any nation [1]. This issue is more serious in electronic based systems. The level of harmonics and reactive power demand are popular parameters that specify the degree of distortion and reactive power demand at a particular bus of the utility [2]. The harmonic resonance is one of the most common problems reported in low- and medium-level distribution systems. It is due to capacitors which are used for power factor correction (PFC) and source impedance [3]. Power converter-based custom power devices (CPDs) are useful for the reduction of power quality problems such as PFC, harmonic compensation, voltage sag/swell compensation, resonance due to distortion, and voltage flicker reduction within specified international standards [4]–[6]. These CPDs include the distribution static compensator (DSTATCOM), dynamic voltage restorer, and unified power quality conditioner in different configurations [7]–[9]. Some of their new topologies are also reported in the literature such as the indirect matrix converterbased active compensator where the dc-link capacitor can be removed [10]. Other new configurations are based on stacked multicell converters where the main features are on the increase in the number of output voltage levels, without transformer operation and natural self-balancing of flying capacitor voltage, etc. [11]. The performance of any custom power device depends very much upon the control algorithm used for the reference current estimation and gating pulse generation scheme. Some of the classical control algorithms are the Fryze power theory, Budeanu

theory, p-q theory and SRF theory [12]–[14], Lyapunov-function-based control [15] and nonlinear control technique [16], etc. Many nonmodel and training-based alternative control algorithms are reported in the literature with application of soft computing technique such as neural network, fuzzy logic and adaptive neuro-fuzzy, etc. [17]–[20]. Adaptive learning, selforganization, real-time operation, and fault tolerance through redundant information are major advantages of these algorithms. A neural network-based control algorithm such as the Hopfield-type neural network is also used for the estimation of the amplitude and phase angles of the fundamental component both with highly distorted voltage by the assumption of known power frequency [21]. An improved adaptive detecting approach for the extraction of the error signal with variable learning parameters can be chosen for fast response to improve tracking speed and for a low value in a stable period to improve accuracy [22]. Wu *et al.* [23] have proposed a new control algorithm based on inverse control with a neural network interface which was applied for the instantaneous calculation of switching on–off time in a digital environment. A survey on iterative learning control (ILC) is presented by Ahn *et al.* [24], and it is classified into different subsections within the wide range of application. The main idea of ILC is to find an input sequence such that the output of the system is as close as possible to a desired output. Control algorithms reported in available texts such as the quantized Kernel least mean square algorithm [25], radial basis function (RBF) networks [26], and feed forward training [27] can also be used for the control of CPDs. An immune RBF neural network integrates the immune algorithm with the RBF neural network. This algorithm has the advantages in the learning speed and accuracy of the astringent signal. Therefore, it can detect the harmonics of the current timely and precisely in the power network [28]. A multilayer perceptron neural network is useful for the identification of nonlinear characteristics of the load. The main advantage of this method is that it requires only waveforms of voltages and currents. A neural network with memory is used to identify the nonlinear load admittance. Once training is achieved, the neural network predicts the true harmonic current of the load when supplied with a clean sine wave. Its application with SRF theory is described by Mazumdar *et al.* [29],[30]. Feed forward back propagation (BP) artificial neural network (ANN) consists of various layers such as the input layer, hidden layer, and output layer. It is based on feed forward BP with a high ability to deal with complex nonlinear problems[31]. The BP control algorithm is also used to design the pattern classification model based on decision support system. The standard BP model has been used with the full connection of each node in the layers from input to the output layers. Some applications of this algorithm are as to the identification of user faces, industrial processes, data analysis, mapping data, control of power quality improvement devices, etc. [32]. The control of power quality devices by neural network is a latest research area in the field of power engineering. The extraction of harmonic component-ts decides the performance of compensating devices. The BP algorithm which trained the sample can detect the signal of the power quality problem in real time. Its simulation study for harmonic detection is presented in [33]. Many neural network-based algorithms are reported with theoretical analysis in single phase system, but their implementation to DSTATCOM is hardly reported in the available literature. In this paper, a BP algorithm is implemented in a three phase shunt connected custom power device known as DSTATCOM for the extraction of the weighted value of load active power and reactive power current components in nonlinear loads. The proposed control algorithm is used for harmonic suppression and load balancing in PFC and zero voltage regulation (ZVR) modes with dc voltage regulation of DSTATCOM. In this BP algorithm, the training of weights has three stages. It includes the feed forward of the input signal training, calculation and BP of the error signals, and upgrading of training weights. It may have one or more than one layer. Continuity, differentiability, and non decreasing monotony are the main characteristics of this algorithm. It is based on a mathematical formula and does not need special features of function in the learning process. It also

has smooth variation on weight correction due to batch updating features on weights. In the training process, it is slow due to more number of learning steps, but after the training of weights, this algorithm produces very fast trained output response. In this application, the proposed control algorithm on a DSTATCOM is implemented for the compensation of nonlinear loads.

II. SYSTEM CONFIGURATION AND CONTROL ALGORITHM

A voltage source converter (VSC)-based DSTATCOM is connected to a three phase ac mains feeding three phase linear/nonlinear loads with internal grid impedance which is shown in Fig. 1. The performance of DSTATCOM depends upon the accuracy of harmonic current detection. For reducing ripple in compensating currents, the tuned values of interfacing inductors (*Lf*) are connected at the ac output of the VSC. A three phase series combination of capacitor (*Cf*) and a resistor (*Rf*) represents the shunt passive ripple filter which is connected at a point of common coupling (PCC) for reducing the high frequency switching noise of the VSC. The DSTATCOM currents (*iCabc*) are injected as required compensating currents to cancel the reactive power components and harmonics of the load currents so that loading due to reactive power component/ harmonics is reduced on the distribution system. For the considered three phase nonlinear load with approximately 24 kW, the compensator data are given in Appendix A.

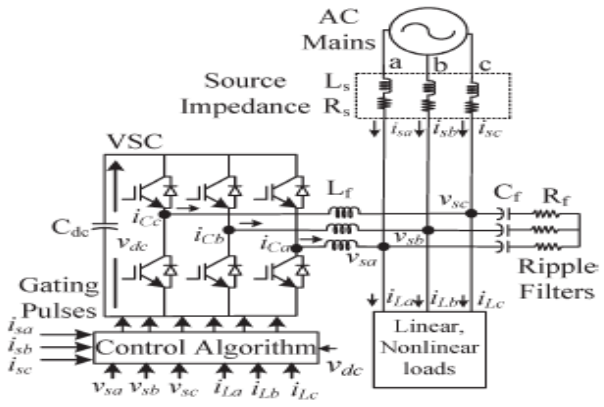

Fig. 1. Schematic diagram of VSC-based DSTATCOM.

Fig. 2 shows the block diagram of the BP training algorithm for the estimation of reference source currents through the weighted value of load active power and reactive power current components. In this algorithm, the phase PCC voltages (*vsa*, *vsb*, and *vsc*), source currents (*isa*, *isb*, and *isc*), load currents (*iLa*, *iLb*, and *iLc*) and dc bus voltage (*vdc*) are required for the extraction of reference source currents There are two primary modes for the operation of this algorithm: The first one is a feed forward, and the second is the BP of error or supervised learning. The detail application of this algorithm for the estimation of various control parameters is given as follows.

A. Estimation of Weighted Value of Average Fundamental Load Active and Reactive Power Components

A BP training [32],[33] algorithm is used to estimate the three phase weighted value of load active power current components (*wap*, *wbp*, and *wcp*) and reactive power current components (*waq*, *wbq*, and *wcq*) from polluted load currents using the feedforward and supervised principle. In this estimation, the input layer for three phases (a, b, and c) is expressed as

$$I_{L_{ap}} = w_{0+} i_{La} u_{ap} + i_{Lb} u_{bp} + i_{Lc} u_{cp} \quad (1)$$

$$I_{L_{bp}} = w_{0+} i_{Lb} u_{bp} + i_{Lc} u_{cp} + i_{La} u_{ap} \quad (2)$$

$$I_{L_{cp}} = w_{0+} i_{Lc} u_{cp} + i_{La} u_{ap} + i_{Lb} u_{bp} \quad (3)$$

where *wo* is the selected value of the initial weight and *uap*, *ubp*, and *ucp* are the in-phase unit templates. In-phase unit templates are estimated using sensed PCC phase voltages (*vsa*, *vsb*, and *vsc*). It is the relation of the phase voltage and the amplitude of the PCC voltage (*vt*). The amplitude of sensed PCC voltages is estimated as

$$v_t = \sqrt{\frac{2(v_{sa}{}^2 + v_{sb}{}^2 + v_{sc}{}^2)}{3}} \quad (4)$$

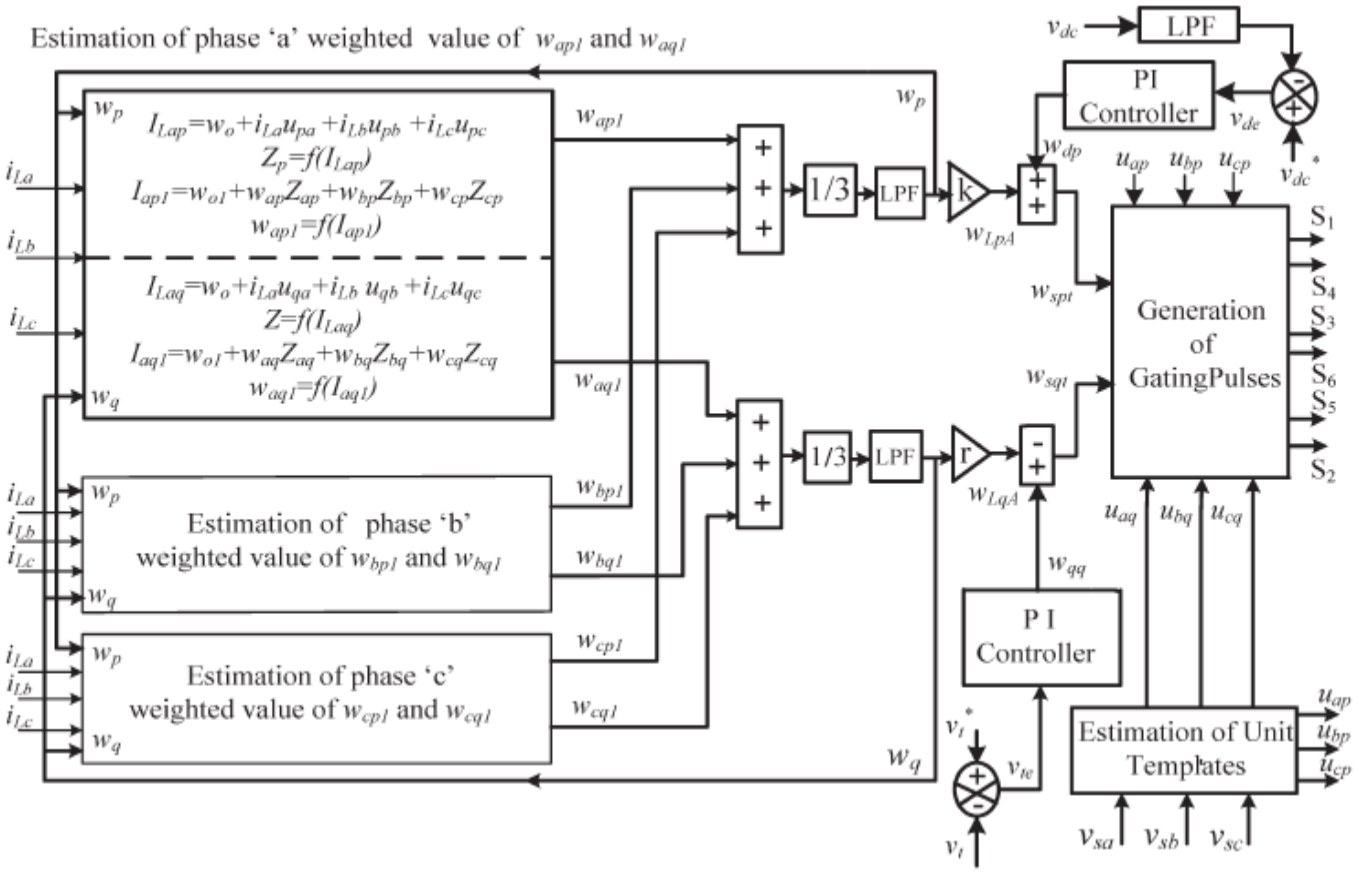

Fig. 2. Estimation of reference currents using BP control algorithm

The in-phase unit templates of PCC voltages (*uap*, *ubp*, and *ucp*) are estimated as [13]

$$u_{ap}=\frac{u_{sa}}{v_t},\quad u_{bp}=\frac{u_{sb}}{v_t},\quad u_{cp}=\frac{u_{sc}}{v_t} \tag{5}$$

The extracted values of $I_{L_{ap}}$, $I_{L_{bp}}$, and $I_{L_{cp}}$ are passed through a sigmoid function as an activation function, and the output signals (*Zap*, *Zbp*, and *Zcp*) of the feedforward section are expressed as

$$Z_{ap}=f(I_{L_{ap}})=\frac{1}{(1+e^{-I_{L_{ap}}})} \tag{6}$$

$$Z_{bp}=f(I_{L_{bp}})=\frac{1}{(1+e^{-I_{L_{bp}}})} \tag{7}$$

$$Z_{cp}=f(I_{L_{cp}})=\frac{1}{(1+e^{-I_{L_{cp}}})} \tag{8}$$

The estimated values of *Zap*, *Zbp*, and *Zcp* are fed to a hidden layer as input signals. The three phase outputs of this layer (*Iap*1, *Ibp*1, and *Icp*1) before the activation function are expressed as

$$I_{ap_1}=w_{0_1}+w_{ap}Z_{ap}+w_{bp}Z_{bp}+w_{cp}Z_{cp} \tag{9}$$

$$I_{bp_1}=w_{0_1}+w_{bp}Z_{bp}+w_{cp}Z_{cp}+w_{ap}Z_{ap} \tag{10}$$

$$I_{cp_1}=w_{0_1}+w_{cp}Z_{cp}+w_{ap}Z_{ap}+w_{bp}Z_{bp} \tag{11}$$

where w_{0_1}, w_{bp}, w_{cp} *and* w_{ap} are the selected value of the initial weight in the hidden layer and the updated values of three phase weights using the average weighted value (*wp*) of the active power current component as a feedback signal, respectively. The updated weight of phase "a" active power current components of load current "*wap*" at the *n*th sampling instant is expressed as

$$w_{ap}(n)=w_p(n)+\mu\{w_p(n)-w_{ap1}(n)\}f'(I_{ap1})Z_{ap}(n) \tag{12}$$

where *wp*(*n*) and *wap*(*n*) are the average weighted value of the active power component of load currents and the updated weighted value of phase "a" at the *n*th sampling instant, respectively, and *wap*1(*n*) and *zap*(*n*) are the phase "a" fundamental

weighted amplitude of the active power component of the load current and the output of the feedforward section of the algorithm at the *n*th instant, respectively. $f\_(Iap1)$ and μ are represented as the derivative of *Iap*1 components and the learning rate. Similarly, for phase "b" and phase "c," the updated weighted values of the active power current components of the load current are expressed as

$$w_{bp}(n) = w_p(n) + \mu\{w_p(n) - w_{bp1}(n)\}f'(I_{bp1})Z_{bp}(n) \quad (13)$$

$$w_{cp}(n) = w_p(n) + \mu\{w_p(n) - w_{cp1}(n)\}f'(I_{cp1})Z_{cp}(n) \quad (14)$$

The extracted values of *Iap*1, *Ibp*1, and *Icp*1 are passed through a sigmoid function as an activation function to the estimation of the fundamental active components in terms of three phase weights *wap*1, *wbp*1, and *wcp*1 as

$$w_{ap1} = f(I_{ap1}) = \frac{1}{(1+e^{-I_{ap1}})} \quad (15)$$

$$w_{bp1} = f(I_{bp1}) = \frac{1}{(1+e^{-I_{bp1}})} \quad (16)$$

$$w_{cp1} = f(I_{cp1}) = \frac{1}{(1+e^{-I_{cp1}})} \quad (17)$$

The average weighted amplitude of the fundamental active power components (*wp*) is estimated using the amplitude sum of three phase load active power components (*wap*1, *wbp*1, and *wcp*1) divided by three. It is required to realize load balancing features of DSTATCOM. Mathematically, it is expressed as

$$w_p = \frac{(w_{ap1}+w_{bp1}+w_{cp1})}{3} \quad (18)$$

First-order low-pass filters are used to separate the low frequency components. "k" denotes the scaled factor of the extracted active power components of current in the algorithm which is shown in Fig. 2. After separating the low-frequency components and scaling to the actual value because the output of the activation function is between 0 and 1, it is represented as *wLpA*. Similarly, the weighted amplitudes of the reactive power components of the load currents (*waq*, *wbq*, and *wcq*) of the fundamental load current are extracted as

$$I_{L_{aq}} = w_{0+} i_{La} u_{aq} + i_{Lb} u_{bq} + i_{Lc} u_{cq} \quad (19)$$

$$I_{L_{bq}} = w_{0+} i_{Lb} u_{bq} + i_{Lc} u_{cq} + i_{La} u_{aq} \quad (20)$$

$$I_{L_{cq}} = w_{0+} i_{Lc} u_{cq} + i_{La} u_{aq} + i_{Lb} u_{bq} \quad (21)$$

where *wo* is the selected value of the initial weight and *uaq*, *ubq*, and *ucq* are the quadrature components of the unit template. The quadrature unit templates (*uaq*, *ubq*, and *ucq*) of the phase PCC voltage are estimated using (5) as

$$u_{aq} = \frac{(-u_{bp}+u_{cp})}{\sqrt{3}}, \quad u_{bq} = \frac{(3u_{ap}+u_{bp}-u_{cp})}{2\sqrt{3}}, \quad u_{cq} = \frac{(-3u_{ap}+u_{bp}-u_{cp})}{2\sqrt{3}} \quad (22)$$

The extracted values of *ILaq*, *ILbq*, and *ILcq* are passed through a sigmoid function as an activation function to the estimation of

$$Z_{aq} = f(I_{L_{aq}}) = \frac{1}{(1+e^{-I_{L_{aq}}})} \quad (23)$$

$$Z_{bq} = f(I_{L_{bq}}) = \frac{1}{(1+e^{-I_{L_{bq}}})} \quad (24)$$

$$Z_{cq} = f(I_{L_{cq}}) = \frac{1}{(1+e^{-I_{L_{cq}}})} \quad (25)$$

The estimated values of *Zaq*, *Zbq*, and *Zcq* are fed to the hidden layer as input signals. The three phase outputs of this layer (*Iaq*1, *Ibq*1, and *Icq*1) before the activation function can be represented as

$$I_{aq_1} = w_{0_1} + w_{aq}Z_{aq} + w_{bq}Z_{bq} + w_{cq}Z_{cq} \quad (26)$$

$$I_{bq_1} = w_{0_1} + w_{bq}Z_{bq} + w_{cq}Z_{cq} + w_{aq}Z_{aq} \quad (27)$$

$$I_{cq_1} = w_{0_1} + w_{cq}Z_{cq} + w_{aq}Z_{aq} + w_{bq}Z_{bq} \quad (28)$$

where *wo*1, *waq*, *wbq*, and *wcq* are the selected value of the initial weight in the hidden layer and the updated three weights using the average weighted value of the reactive power components of currents (*wq*) as a feedback signal, respectively. The updated weight of the phase "a" reactive power components of load currents "*waq*" at the *n*th sampling instant is expressed as

$$w_{aq}(n) = w_q(n) + \mu\{w_q(n) - w_{aq1}(n)\}f'(I_{aq1})Z_{aq}(n) \quad (29)$$

wq(*n*) and *waq*(*n*) are the average weighted value of the reactive power component of load currents and the updated weight in the *n*th sampling instant, respectively, and *waq*1(*n*) and *zaq*(*n*) are the phase

"a" weighted amplitude of the reactive power current component of load currents and the output of the feedforward section of the algorithm at the *n*th instant, respectively. $f\_(Iaq1)$ and μ are presented as the derivative of *Iaq*1 components and the learning rate. Similarly, for phase "b" and phase "c," the updated weighted values of the reactive power current components of the load current are expressed as

$$w_{bq}(n) = w_q(n) + \mu\{w_q(n) - w_{bq1}(n)\}f'(I_{bq1})Z_{bq}(n) \quad (30)$$

$$w_{cq}(n) = w_q(n) + \mu\{w_q(n) - w_{cq1}(n)\}f'(I_{cq1})Z_{cq}(n) \quad (31)$$

The extracted values of *Iaq*1, *Ibq*1, and *Icq*1 are passed through an activation function to the estimation of the fundamental reactive component in terms of three phase weights *waq*1, *wbq*1, and *wcq*1 as

$$w_{aq1} = f(I_{aq1}) = \frac{1}{(1+e^{-I_{aq1}})} \quad (32)$$

$$w_{bq1} = f(I_{bq1}) = \frac{1}{(1+e^{-I_{bq1}})} \quad (33)$$

$$w_{cq1} = f(I_{cq1}) = \frac{1}{(1+e^{-I_{cq1}})} \quad (34)$$

The average weight of the amplitudes of the fundamental reactive power current components (*wq*) is estimated using the amplitude sum of the three phase load reactive power components of the load current (*waq*1, *wbq*1, and *wcq*1) divided by three. Mathematically, it is expressed as

$$w_q = \frac{(w_{aq1}+w_{bq1}+w_{cq1})}{3} \quad (35)$$

First-order low-pass filters are used to separate the low frequency component. "r" denotes the scaled factor of the extracted reactive power components in the algorithm which is shown in Fig. 2. After separating low-frequency components and scaling to the actual value because the output of the activation function is between 0 and 1, it is represented as *wLqA*.

B. Amplitude of Active Power Current Components of Reference Source Currents

An error in the dc bus voltage is obtained after comparing the reference dc bus voltage $v*\ dc$ and the sensed dc bus voltage *vdc* of a VSC, and this error at the *n*th sampling instant is expressed as

$$v_{dc}(n) = v_{dc}(n)^* - v_{dc}(n) \quad (36)$$

This voltage error is fed to a proportional–integral (PI) controller whose output is required for maintaining the dc bus At the *n*th sampling instant, the output of the PI controller is as follows:

$$w_{dp}(n) = w_{dp}(n-1) + k_{pd}\{v_{dc}(n) - vdc(n-1) + kidvdc(n) \quad (37)$$

where *kpd* and *kid* are the proportional and integral gain constants of the dc bus PI controller. *vde*(*n*) and *vde*($n-1$) are the dc bus voltage errors in the *n*th and ($n-1$)th instant, and *wdp*(*n*) and *wdp*($n-1$) are the amplitudes of the active power component of the fundamental reference current at the *n*th and ($n-1$)th instant, respectively. The amplitude of the active power current components of the reference source current (*wspt*) is estimated by the addition of the output of the dc bus PI controller (*wdp*) and the average magnitude of the load active currents (*wLpA*) as

$$w_{spt} = w_{dp} + w_{LPA} \quad (38)$$

C. Amplitude of Reactive Power Components of Reference

Source Currents An error in the ac bus voltage is achieved after comparing the amplitudes of the reference ac bus voltage $v*\ t$ and the sensed ac bus voltage *vt* of a VSC. The extracted ac bus voltage error *vte* at the *n*th sampling instant is expressed as

$$v_{tc}(n) = v_{tc}(n)^* - v_{tc}(n) \quad (39)$$

The weighted output of the ac bus PI controller *wqq* for regulating the ac bus terminal voltage at the *n*th sampling instant is expressed as

$$w_{qq}(n) = w_{qq}(n-1) + k_{pt}\{v_{tc}(n) - v_{tc}(n-1)\} + k_{it}v_{tc}(n) \quad (40)$$

where *wqq*(*n*) is part of the reactive power component of the source current and it is renamed as *wqq*. *kpt* and *kit* are the proportional and integral gain constants of the ac bus voltage PI controller. The amplitude of the reactive power current components of the reference source current (*wsqt*) is calculated by subtracting the output of the voltage PI controller (*wqq*) and the average load reactive currents (*wLqA*) as

$$w_{sqt} = w_{qq} - w_{LqA} \quad (41)$$

D. Estimation of Reference Source Currents and Generation of IGBT Gating Pulses

Three phase reference source active and reactive current components are estimated using the amplitude of three phase (a, b, and c) load active power current components, PCC voltage in-phase unit templates, reactive power current components, and PCC quadrature voltage unit templates as

$$i_{sap} = w_{spt}u_{ap}, i_{sbp} = w_{spt}u_{bp}, i_{scp} = w_{spt}u_{cp} \quad (42)$$

$$i_{saq} = w_{sqt}u_{aq}, i_{sbq} = w_{sqt}u_{bq}, i_{scp} = w_{sqt}u_{cq} \quad (43)$$

Supply voltage

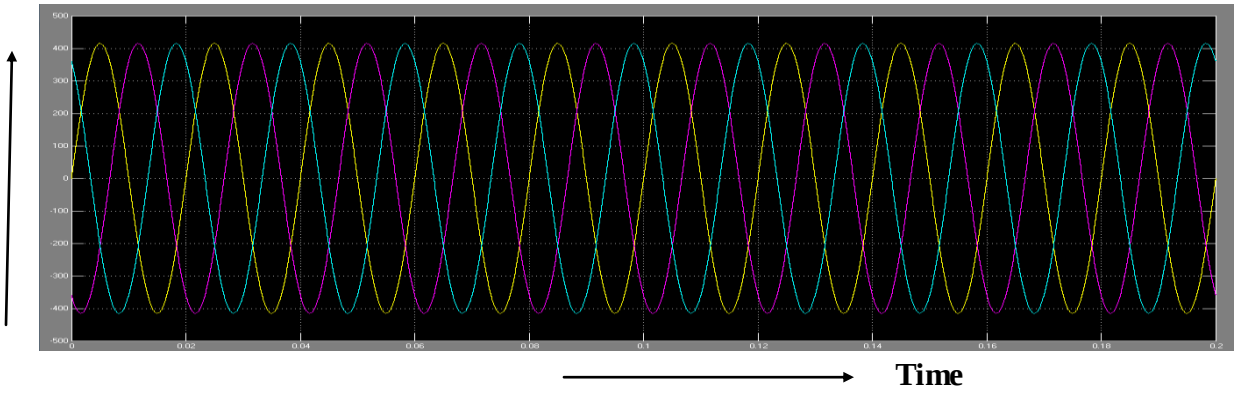

Fig. 3.a Simulation result for the supply voltage in PFC mode

Source currents

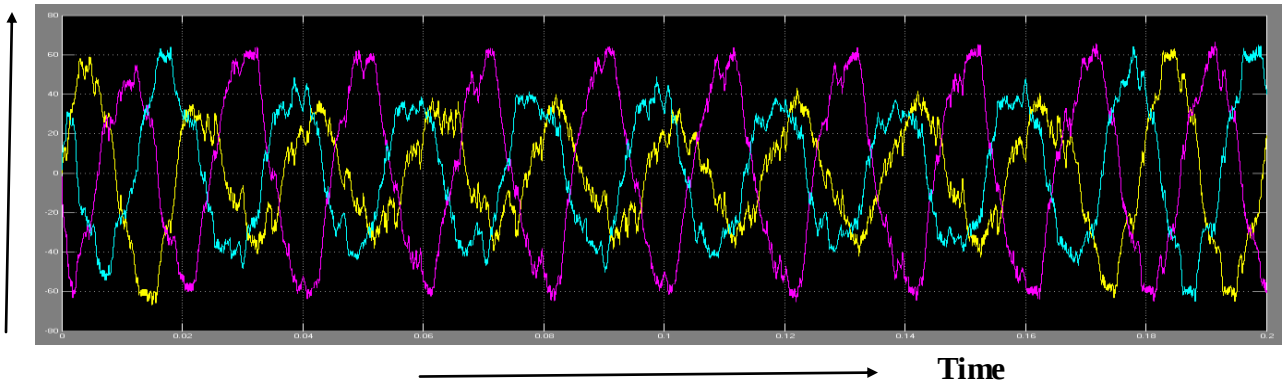

Fig. 3.b Simulation result for the Source currents in PFC

Load currents($i_{l_a}, i_{l_b}, i_{l_c}$)

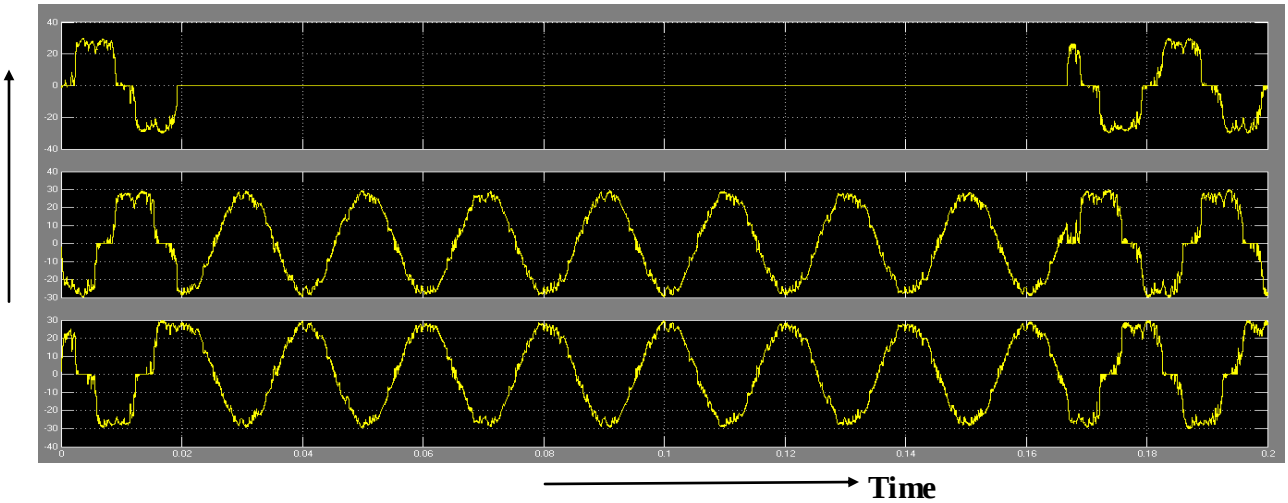

Fig. 3.c Simulation result for the load currents in PFC

Compensator currents ($i_{c_a}, i_{c_b}, i_{c_c}$)

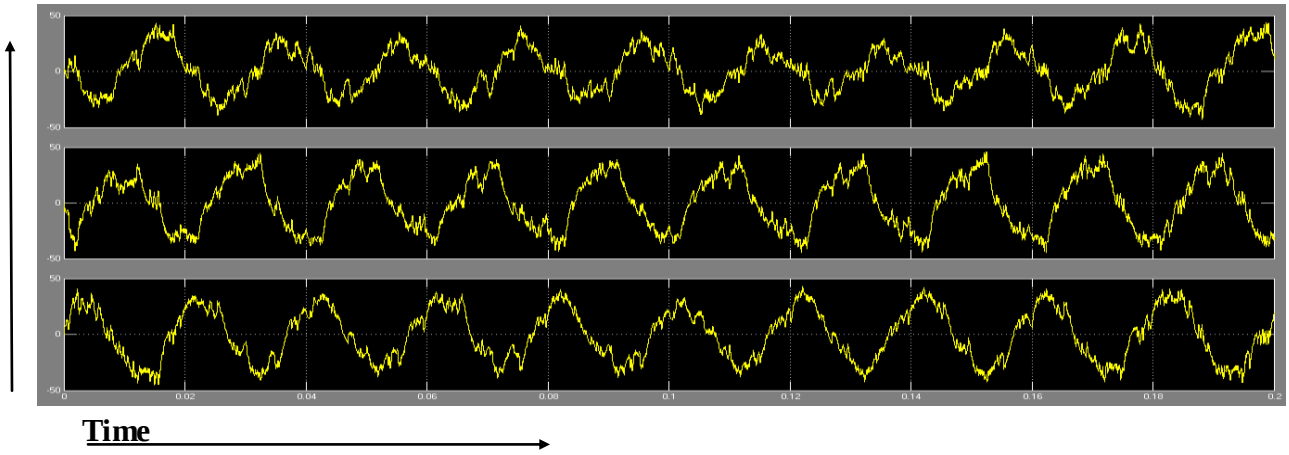

Fig. 3.d Simulation result for the Compensator currents in PFC

DC bus voltage

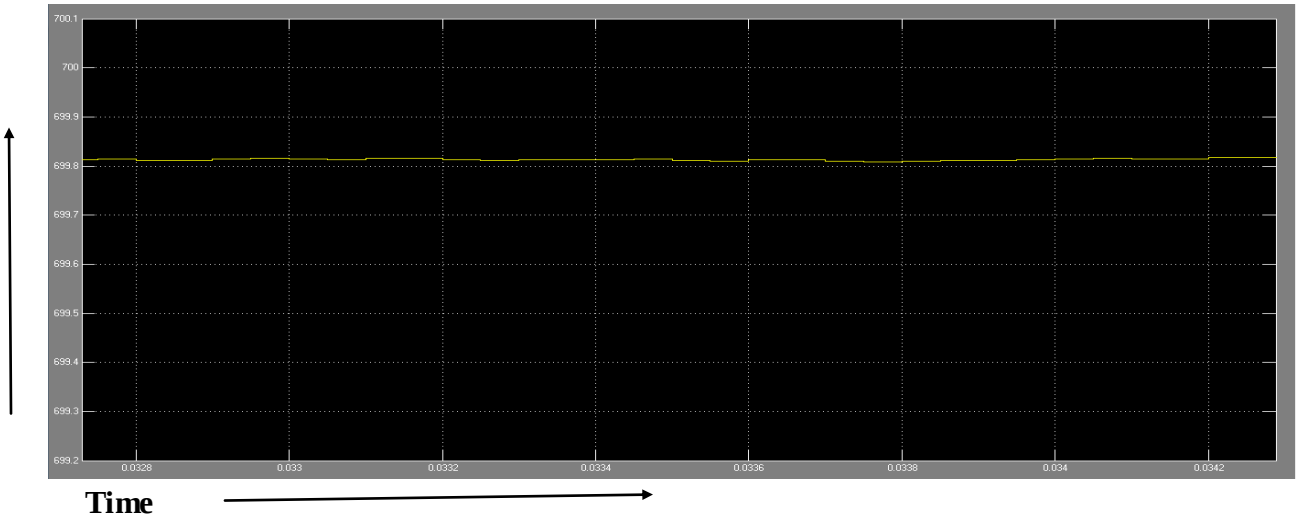

Fig. 3.e Simulation result for the DC bus voltage in PFC mode

Fig. 3. Dynamic performance of DSTATCOM under varying nonlinear loads in PFC mode

The addition of reference active and reactive current components is known as reference source currents, and these are given as

$i_{sa}{}^{*} = i_{sap} + i_{saq}$, $i_{sb}{}^{*} = i_{sbp} + i_{sbq}$, $i_{sc}{}^{*} = i_{scp} + i_{scq}$ ---------- (44)

The sensed source currents (*isa, isb, isc*) and the reference source currents (*i*sa, i*sb, i*sc*) are compared, and current error signals are amplified through PI current regulators; their outputs are fed to a pulse width modulation (PWM) controller to generate the gating signals for insulated-gate bipolar transistors (IGBTs) S1 to S6 of the VSC used as a DSTATCOM.

III. SIMULATION RESULTS AND DISCUSSION

MATLAB with SIMULINK and Sim Power System toolboxes is used for the development of the simulation model of a DSTATCOM and its control algorithm. The performance of the BP algorithm in the time domain for the three phase DSTATCOM is simulated for PFC and ZVR modes of operation under nonlinear loads. The performance of the control algorithm is observed under nonlinear loads.

A. Performance of DSTATCOM in PFC Mode

The dynamic performance of a VSC-based DSTATCOM is studied for PFC mode at nonlinear loads. The performance indices are the phase

voltages at PCC (*vs*), balanced source currents (*is*), load currents (*iLa*, *iLb*, and *iLc*), compensator currents (*iCa*, *iCb*, and *iCc*), and dc bus voltage (*vdc*) which are shown in Fig. 3 under varying load (at t = 3.7 to 3.8 s)conditions.The total harmonic distortion (THD) of the phase "a" at PCC voltage, source current, and load current are found to be 2.86%, 2.94%, and 24.82%, respectively. It is observed that the DSTATCOM is able to perform the functions of load balancing and harmonic elimination with high precision.

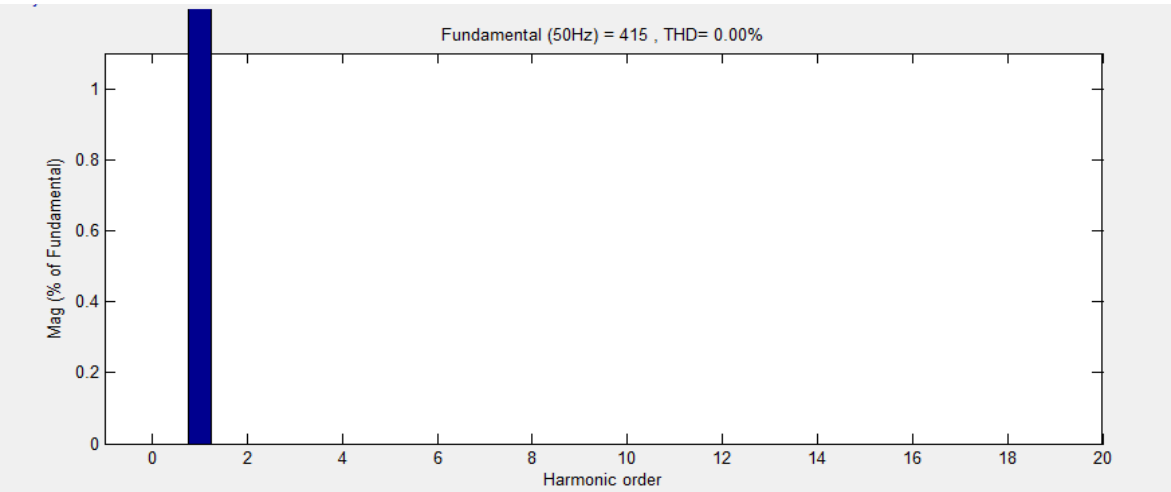

Fig. 4.a Harmonic spectra for the supply voltage in ZVR mode

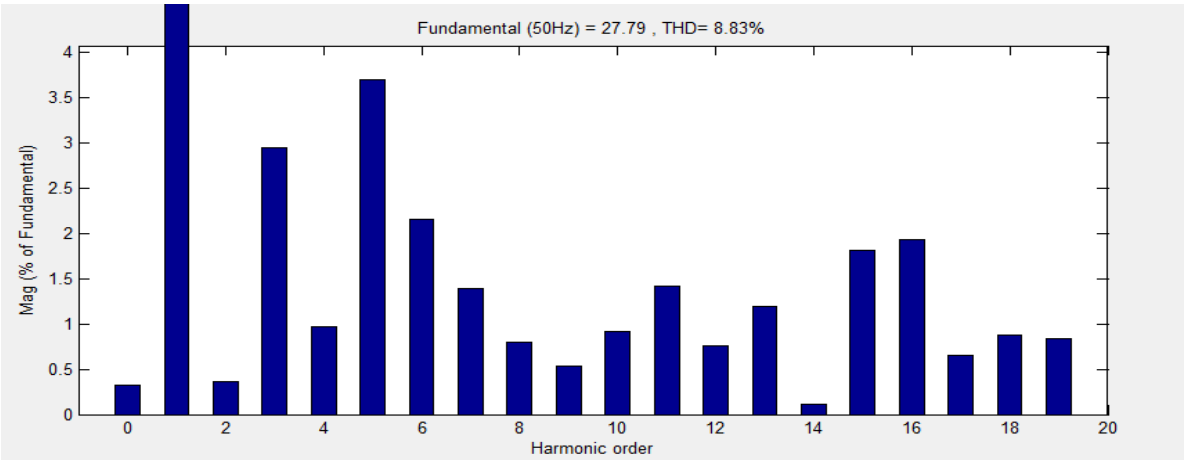

Fig. 4.b Harmonic spectra for the load current in PFC mode

Fig. 4. Waveforms and harmonic spectra in PFC mode

B. Performance of DSTATCOM in ZVR Mode

In ZVR mode, the amplitude of the PCC voltage is regulated to the reference amplitude by injecting extra leading reactive power components. The dynamic performance of DSTATCOM in terms of PCC phase voltages (*vs*), balanced source currents (*is*), load currents (*iLa*, *iLb*, and *iLc*), compensator currents (*iCa*, *iCb*, and *iCc*), amplitude of voltages at PCC (*vt*), and dc bus voltage (*vdc*) waveforms is shown in Fig. 5 under unbalanced load at a time duration of t = 3.7 to 3.8 s. The harmonic spectra of the phase "a" voltage at PCC (*vsa*), source current (*isa*), and load current (*iLa*) are shown in Fig. 6(a)–(c). The THDs of the phase "a" at PCC voltage, source current, load current are observed to be 3.09%, 2.99%, and 24.94%, respectively. Three phase PCC voltages are regulated up to the rated value. The amplitude of the three phase voltages is regulated from 335.2 to 338.9 V under nonlinear loads. It may be seen that the harmonic distortions of the source current and PCC voltage are within the IEEE-519 standard limit of 5%. The PCC voltage is also regulated at different operating conditions of load. Table I shows the summarized simulation

results demonstrating the performance of DSTATCOM. These results show satisfactory performance of DSTATCOM for harmonicelimination and load balancing of nonlinear loads.

IV. EXPERIMENTAL RESULTS

A prototype of the VSC-based DSTATCOM is developed to validate the proposed control algorithm. ABB make current sensors (EL50P1 BB) and voltage sensors (EM010 BB) are used for sensing the PCC voltages, dc bus voltage, and current signals. The BP training-based control algorithm is used for the control of DSTATCOM using a TMS320F240 digital signal processor. A Fluke (43B) power analyzer and an Agilent make digital oscilloscope (DSO-6014A) are used for the recording of steady state and dynamic state test results, respectively, on a developed DSTATCOM at nonlinear loads. Hardware implementation data are given in Appendix B.

Supply voltage

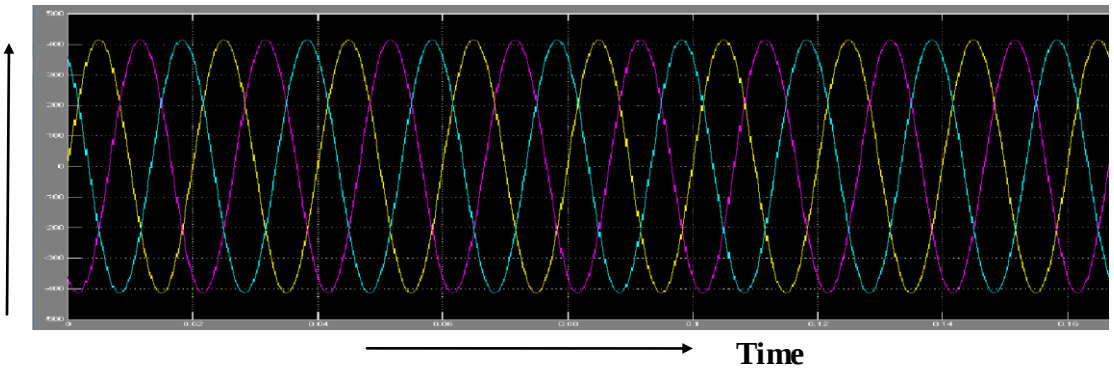

Fig. 5.a Simulation result for the supply voltage in ZVR mode

Source currents

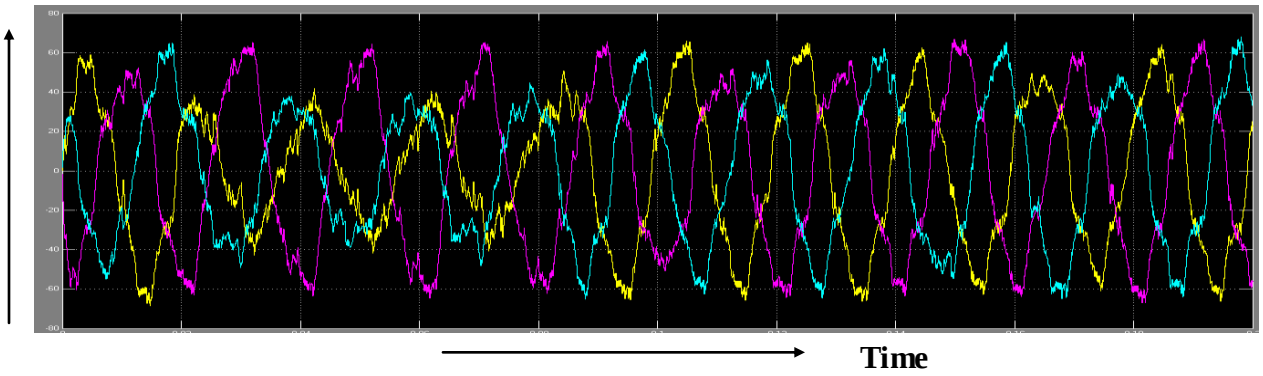

Fig. 5.b Simulation result for the source currents in ZVR mode

Load currents($i_{l_a}, i_{l_b}, i_{l_c}$)

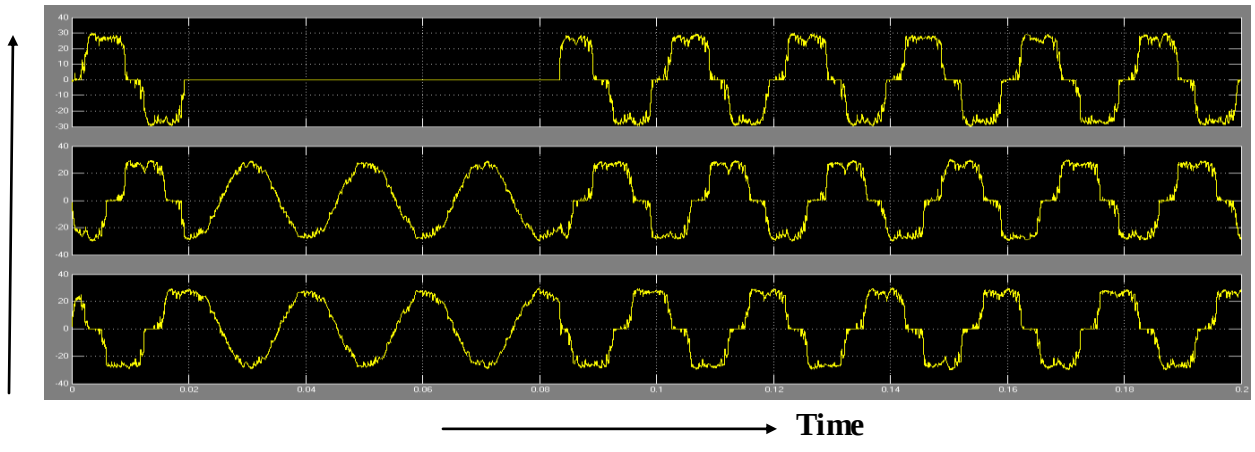

Fig. 5.c Simulation results for the load currents for the three phases in ZVR mode

Compensator currents ($i_{c_a}, i_{c_b}, i_{c_c}$)

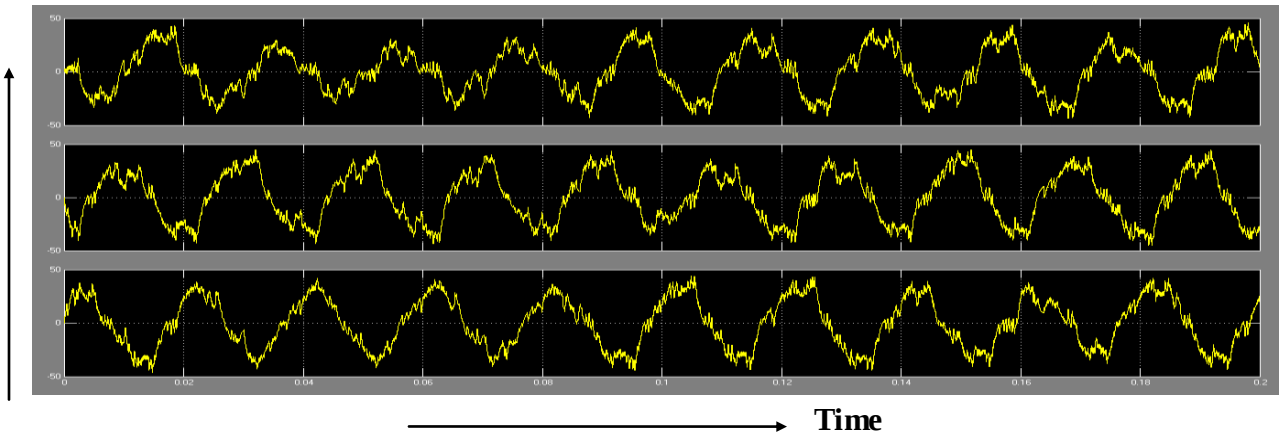

Fig. 5.d Simulation results for the compensator currents in ZVR mode

Dc bus voltage

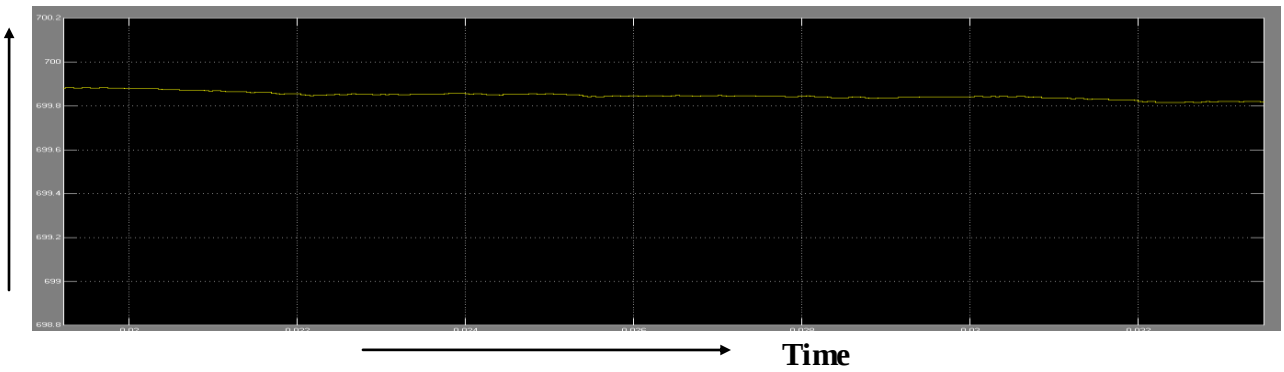

Fig. 5.e Simulation result for the DC bus voltage in ZVR mode

Fig. 5. Dynamic performance of DSTATCOM under varying nonlinear loads in ZVR mode

A. Performance of DSTATCOM at Nonlinear Loads

Fig. 7(a)–(i) shows the waveform of the phase "a" PCC voltage (*vab*) with source currents (*isa*, *isb*, and *isc*), load currents (*iLa*, *iLb*, and *iLc*), and compensating current (*iCa*, *iCb*, and *iCc*) under nonlinear loads. PCC voltage are observed to be 4.3%, 27.0%,and 2.9%, respectively. These results show satisfactory performance of the BP control algorithm for harmonic elimination according to the IEEE-519 guidelines on the order of less than 5%.

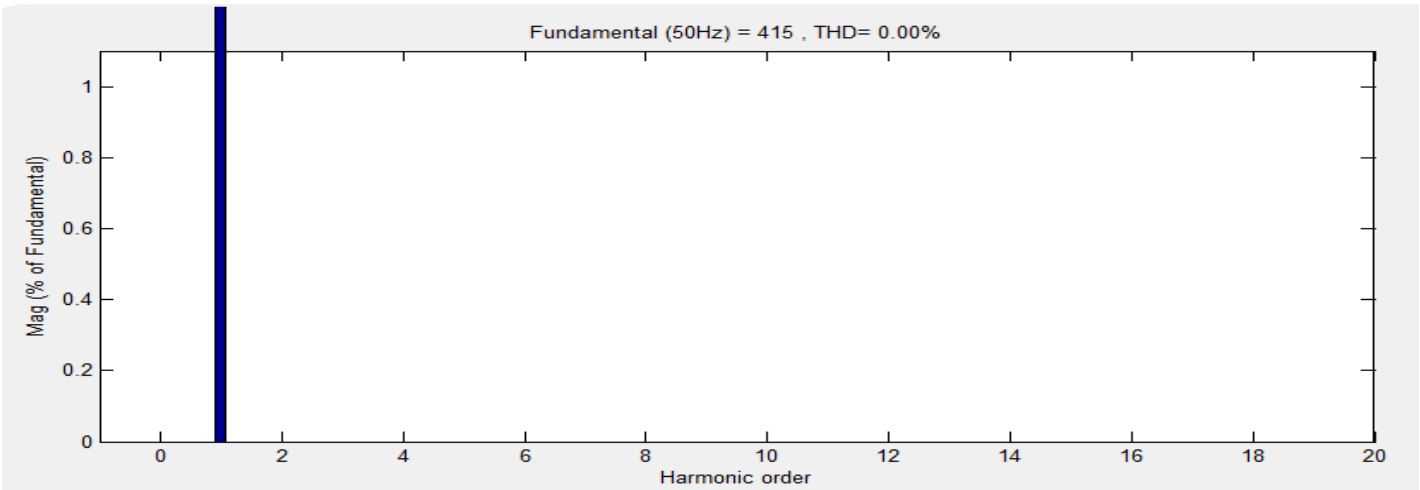

Fig. 6.a Harmonic spectra for the supply voltage in ZVR mode

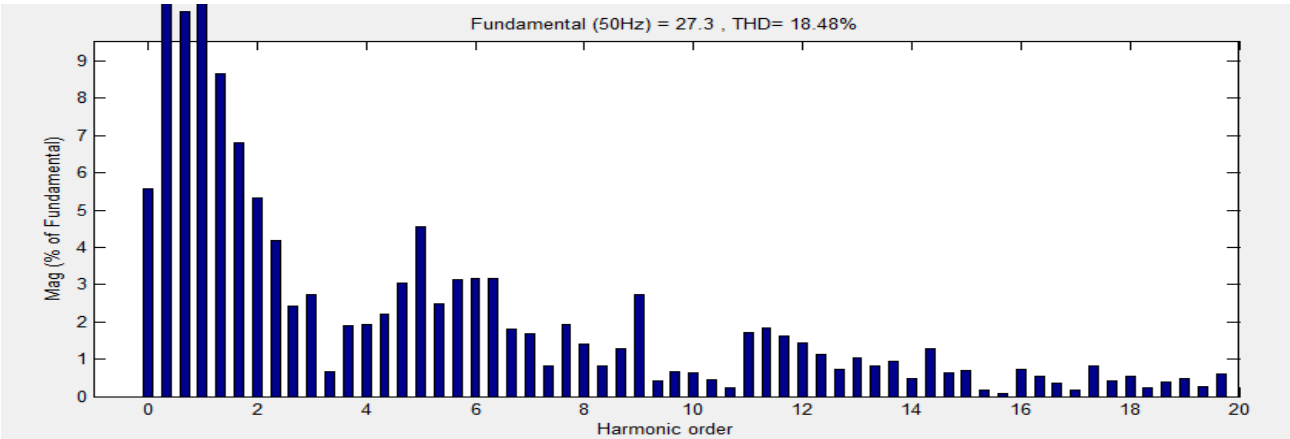

Fig. 6.b Harmonic spectra for the load current in ZVR mode

Fig. 6. Waveforms and harmonic spectra of in ZVR mode

Table I Performance of Dstatcom

Operating mode	Performance parameters	Non linear load (3-phase un controlled rectifier with R and L load)
PFC mode	PCC voltage (V),%THD	237.02V,2.86%
	Supply current (A),%THD	32.17A, 2.94%
	Load current (A),%THD	32.58A,24.82%
ZVR mode	PCC voltage(v),%THD	239.63V,3.09%
	Source current(A),%THD	33.82A,2.99%
	Load current(A),%THD	32.94A,24.94%
	Dc bus voltage	700V

B. Dynamic Performance of DSTATCOM

the waveform of the source currents (*isa*, *isb*, and *isc*), load currents (*iLa*, *iLb*, and *iLc*), and compensating currents (*iCa*, *iCb*, and *iCc*) with PCC line voltage (*vab*) under unbalanced nonlinear loads. Unbalanced loads can be observed before load injection in phase "a." The variation of dc bus voltage (*vdc*) and PCC voltage with source current (*isa*), load current (*iLa*), and compensating current (*iCa*) is shown in Fig. 8(d) and (e). The variation of dc bus voltage (*vdc*) and PCC voltage with source current (*isa*), load current (*iLa*), and compensating current (*iCa*) during load removal is shown in Fig. 9(a) and (b). These results show balanced source currents when load currents are not balanced, and it proves the fast action of the control algorithm after load injection. These results show the acceptable performance of the control algorithm of DSTATCOM under unbalanced nonlinear loads.

V. CONCLUSION

A VSC-based DSTATCOM has been accepted as the most preferred solution for power quality improvement as PFC and to maintain rated PCC voltage. A three phase DSTATCOM has been implemented for the compensation of nonlinear loads us- ing a BPT control algorithm to verify its effectiveness. The proposed BPT control algorithm has been used for the extraction of reference source currents to generate the switching pulses for IGBTs of the VSC of DSTATCOM. Various functions of DSTATCOM such as harmonic elimination and load balancing have been demonstrated in PFC and ZVR modes with dc voltage regulation of DSTATCOM. From the simulation and implementation results, it is concluded that DSTATCOM and its control algorithm have been found suitable for the compensation of nonlinear loads. Its performance has been found satisfactory for this application because the extracted reference source currents exactly traced the sensed source currents during the steady state as well as dynamic conditions. The dc bus voltage of the DSTATCOM has also been regulated to the rated value without any overshoot or undershoot during load variation. Large training time in the application of the complex system and the selection of the number of hidden layers in the system are the disadvantages of this algorithm.

APPENDIX A

AC supply source: three-phase, 415 V (L-L), 50 Hz. Source impedance: *Rs* = 0.04 Ω and *Ls* = 2 mH. Nonlinear: three phase full bridge uncontrolled rectifier with *R* = 13Ωand *L* = 200 mH. Rating of VSC = 10 kVA (approximately 30% higher than the rated value). Ripple filter: *Rf* = 5Ωand *Cf* = 10 μF. Switching frequency of inverter = 10 kHz. Reference dc bus voltage: 700 V. Interfacing inductor (*Lf*) = 2.75 mH. Gains of PI controller for dc bus voltage: *kpd* = 3.1 and *kid* = 0.9. Gains of voltage PI controller: *kpt* = 2.95 and *kit* = 4. Selected initial weights: *wo* = 0.4 and *wo*1 = 0.2. Learning rate (μ) = 0.6. Cutoff frequency of low-pass filter used in dc bus voltage = 15 Hz. Cutoff frequency of low-pass filter used in ac bus voltage = 10 Hz.

APPENDIX B

AC supply source: three-phase, 225 V (L-L), 50 Hz. Nonlinear loads: three phase full bridge uncontrolled rectifier with *R* = 43 Ω and *L* = 200 mH. DC bus capacitance: 1650 μF. Reference dc bus voltage: 400 V. Interfacing inductor (*Lf*) = 3 mH. Ripple filter: *Rf* = 5 Ω and *Cf* = 10 μF. Cutoff frequency of low-pass filter used in dc bus = 15 Hz. Selected initial weights: *wo* = 0.4 and *wo*1 = 0.2. Learning rate (μ) = 0.6. Sampling time with used digital plate from *ts* = 50 μs.

REFERENCES

1. R. C. Dugan, M. F. McGranaghan, and H. W. Beaty, *Electric Power Systems Quality*, 2nd ed. New York, NY, USA: McGraw-Hill, 2006.
2. A. Ortiz, C. Gherasim, M. Manana, C. J. Renedo, L. I. Eguiluz, and R. J. M. Belmans, "Total harmonic distortion decomposition depending on distortion origin,"*IEEE Trans. Power Del.*,v 20, no 4, pp.2651-2656,Oct 05.
3. T. L. Lee and S. H. Hu, "Discrete frequency-tuning active filter to suppress harmonic resonances of closed-loop distribution power systems," *IEEE Trans. Power Electron.*, vol. 26, no. 1, pp.137–148, Jan. 2011. 1212 IEEE Transactions On Industrial Electronics, Vol. 61, No. 3, March 2014
4. K. R. Padiyar, *FACTS Controllers in Power Transmission and Distribution*. New Delhi, India: New Age Int., 2008.
5. *IEEE Recommended Practices and Requirement for Harmonic Control on Electric Power System*, IEEE Std.519, 1992.
6. T.-L. Lee, S.-H. Hu, and Y.-H. Chan, "DSTATCOM with positive sequence admittance and negative-sequence conductance to mitigate voltage fluctuations in high-level penetration of distributed generation systems," *IEEE Trans. Ind. Electron.*, vol. 60, no. 4, pp. 1417–1428, Apr. 2013.
7. B. Singh, P. Jayaprakash, and D. P. Kothari, "Power factor correction and power quality improvement in the distribution system," *Elect. India Mag.*, pp. 40–48, Apr. 2008.
8. J.-C. Wu, H. L. Jou, Y. T. Feng, W. P. Hsu, M. S. Huang, and W. J. Hou, "Novel circuit topology for three-phase active power filter," *IEEE Trans. Power Del.*, vol. 22, no. 1, pp. 444–449, Jan. 2007.
9. Z. Yao and L. Xiao, "Control of single-phase grid-connected inverters with nonlinear loads," *IEEE Trans. Ind. Electron.*, vol. 60, no. 4, pp. 1384– 1389, Apr. 2013.
10. A. A. Heris, E. Babaei, and S. H. Hosseini, "A new shunt active power filter based on indirect matrix converter," in *Proc. 20th Iranian Conf. Elect. Eng.*, 2012, pp.581–586.
11. M. Sadeghi, A. Nazarloo, S. H. Hosseini, and E. Babaei, "A new DSTATCOM topology based on stacked multicell conv-erter," in *Proc. 2nd Power Electron., Drive Syst. Technol. Conf.*, 2011, pp. 205–210.
12. G. Benysek and M. Pasko, *Power Theories for Improved Power Quality*. London, U.K.: Springer-Verlag, 2012.
13. B. Singh and J. Solanki, "A comparison of control algorithms for DSTATCOM," *IEEE Trans. Ind. Electron.*, vol. 56, no. 7, pp. 2738–2745, Jul. 2009.
14. C. H. da Silva, R. R. Pereira, L. E. B. da Silva, G. Lambert-Torres, B. K. Bose, and S. U. Ahn, "A digital PLL scheme for three-

phase system using modified synchronous reference frame," *IEEE Trans. Ind. Electron.*, vol. 57, no. 11, pp. 3814–3821, Nov. 2010.

15. S. Rahmani, A. Hamadi, and K. Al-Haddad, "A Lyapunov-function-based control for a three-phase shunt hybrid active filter," *IEEE Trans. Ind. Electron.*, vol. 59, no. 3, pp. 1418–1429, Mar. 2012.
16. S. Rahmani, N. Mendalek, and K. Al-Haddad, "Experimental design of a nonlinear control technique for three-phase shunt active power filter," *IEEE Trans. Ind. Electron.*, vol. 57, no. 10, pp. 3364–3375, Oct. 2010.
17. S. N. Sivanandam and S. N. Deepa, *Principle of Soft Computing*. New Delhi, India: Wiley India Ltd., 2010.
18. J. S. R. Jang, C. T. Sun, and E. Mizutani, *Neuro Fuzzy and Soft Computing: A Computational Approach to Learning and Machine Intelligence*. Delhi, India: Pearson Educ. Asia, 2008.
19. P. Kumar and A. Mahajan, "Soft computing techniques for the control of an active power filter," *IEEE Trans. Power Del.*, vol. 24, no. 1, pp. 452– 461, Jan. 2009.
20. A. Bhattacharya and C. Chakraborty, "A shunt active power filter with enhanced performance using ANN-based predictive and adaptive controllers," *IEEE Trans. Ind. Electron.*, v 58, no 2, pp. 421–428,Feb. 2011.
21. L. L. Lai,W. L. Chan, and A. T. P. So, "A two-ANN approach to frequency and harmonic evaluation," in *Proc. 5th Int. Conf. Artif. Neural Netw.*, 1997, pp. 245–250.
22. X. Mao, "The harmonic currents detecting algorithm based on adaptive neural network," in *Proc. 3rd Int. Symp. Intell. Inf. Technol. Appl.*, 2009, vol. 3, pp. 51–53.
23. J.Wu, H. Pang, and X. Xu, "Neural-network-based inverse controlmethod for active power filter system," in *Proc. IEEE Int. Symp. Intell. Control*, 2006, pp. 3094–3097.
24. H.-S. Ahn, Y. Q. Chen, and K. L. Moore, "Iterative learning control: Brief survey and categorization," *IEEE Trans. Syst., Man, Cybern. C, Appl. Rev.*, vol. 37, no. 6, pp. 1099–1121, Nov. 2007.
25. B. Chen, S. Zhao, P. Zhu, and J. C. Principe, "Quantized kernel least mean square algorithm," *IEEE Trans. Neural Netw. Learn. Syst.*, vol. 23, no. 1, pp. 22–32, Jan. 2012.
26. Y. Hao, X. Tiantian, S. Paszczynski, and B. M. Wilamowski, "Advantages of radial basis function networks for dynamic system design," *IEEE Trans. Ind. Electron.*, vol. 58, no. 12, pp. 5438–5450, Dec. 2011.
27. X. Jing and L. Cheng, "An optimal-PID control algorithm for training feed-forward neural networks," *IEEE Trans. Ind. Electron.*, vol. 60, no. 6, pp. 2273–2283, Jun. 2013.
28. F. Guangjie and Z. Hailong, "The study of the electric power harmonics detecting method based on the immune RBF neural network," in *Proc. 2nd Int. Conf. Intell. Comput. Technol. Autom.*, 2009, vol. 1, pp. 121–124.
29. J. Mazumdar, R. G. Harley, and G. K. Venayagamoorthy, "Synchronous reference frame based active filter current reference generation using neural networks," in *Proc. 32nd IEEE Annu. Conf. Ind. Electron.*, 2006, pp. 4404–4409.
30. J. Mazumdar, R. G. Harley, F. Lambert, and G. K. Venayagamoorthy, "A novel method based on neural networks to distinguish between load harmonics and source harmonics in a power system," in *Proc. IEEE Power Eng. Soc. Inaugural Conf. Expo. Africa*, 2005, pp. 477–484.
31. A. Zouidi, F. Fnaiech, K. Al-Haddad, and S. Rahmani, "Artificial neural networks as harmonic detectors," in *Proc. 32nd Annu. Conf. IEEE Ind. Electron.*, 2006, pp. 2889–2892.
32. I. Jung and G. N. Wang, "Pattern classification of back-propagation algorithm using exclusive connecting network," *J. World Acad. Sci., Eng. Technol.*, vol. 36, pp. 189–193, Dec. 2007.

33. C. Ying and L. Qingsheng, "New research on harmonic detection based on neural network for power system," in *Proc. 3rd Int. Symp. Intell. Inf. Technol. Appl.*, 2009, vol. 2, pp. 113–116.

Author's Profile

Raja. Sai kiran was born in Andhra Pradesh,India. He received the B.Tech degree in Electrical and Electronics Engineering from Narayana Engineering collage Gudur, Andhra Pradesh in 2013 and Pursuing M.Tech degree in Electrical power system from ASIT, Gudur,Andhra Pradesh,India. His areas of interest in the field of power system, electrical machines. Email: *china.sai240@gmail.com*

Mr. M.NAGARAJU was born in Andhra Pradesh, India. He received the B.Tech degree in Electrical and Electronics Engineering from JNT University, Hyderabad in 2002 and M.Tech degree in Electrical Power Systems from JNT University Ananthapur in 2008. He is currently pursuing the Ph.D. degree at the JNT University, Hyderabad, Andhra Pradesh, India. He had worked as an Assistant professor in the Dept of EEE in N.B.K.R.I.S.T Vidyanagar. worked as a Assistant professor in the Dept of EEE in Chadalawada Engg,college, Tirupathi. Worked as lecture in Govt Polytechnic, Gudur. Currently He is working as an Associate Professor at Audisankara Institute of Technology Gudur,AP. He was the academic project coordinator for Under-Graduate & Post Graduate students. His areas of interest are Power Quality, FACTS, Reactive Power Control.
Email: nag707@gmail.com